Letters

A Methodology for Predicting Acoustic Noise From Singing Capacitors in Mobile Devices

Xin Yan, *Graduate Student Member, IEEE*, Jianmin Zhang, *Senior Member, IEEE*, Songping Wu, *Senior Member, IEEE*, Ming-Feng Xue, Chi Kin Benjamin Leung, Eric A. MacIntosh, *Member, IEEE*, and Daryl G. Beetner, *Senior Member, IEEE*

***Abstract*—Multilayer ceramic capacitors (MLCCs) connected to a power distribution network (PDN) can create acoustic noise through a combination of the power rail noise at the MLCCs and the piezoelectric effect of the capacitor's ceramic material. The deformation of the MLCCs brought on by power supply noise creates vibrations which cause the printed circuit board (PCB) to vibrate and generate the audible acoustic noise. In the following paper, a simulation methodology is presented to analyze the acoustic noise created by MLCCs on a PCB. A simulation model for the PCB vibration modal response is built and the modal superposition method is used to analyze the harmonic response of the PCB excited by the capacitor. By multiplying the measured power noise spectrum on the MLCC with the simulated deformation of the PCB found from the harmonic response analysis, the total response is obtained. Simulated results show a good correlation with the measured acoustic noise. The proposed method shows promise for analyzing and predicting the acoustic noise from singing capacitors.**

***Index Terms*—Acoustic noise, harmonic response, modal analysis, multilayer ceramic capacitors, piezoelectric effect.**

I. Introduction

With the rapid advance of high-speed digital devices and their integration throughout society, the demand for multilayer ceramic capacitors (MLCCs) has never been higher. One of the most important applications of MLCCs is as decoupling capacitors for the power distribution network (PDN). MLCCs limit power bus noise, which is necessary to ensure the functionality of integrated circuits (IC) connected to the PDN. The effects of MLCC packaging, placement, and ground via layout on PDN noise have been extensity studied [1], [2].

Manuscript received 14 February 2023; revised 17 April 2023; accepted 12 May 2023. Date of publication 7 June 2023; date of current version 15 August 2023. This work was supported in part by the National Science Foundation (NSF) under Grant IIP-1916535. *(Corresponding author: Xin Yan.)*

Xin Yan and Daryl G. Beetner are with the EMC Laboratory, Missouri University of Science and Technology, Rolla, MO 65409 USA (e-mail: yx9n9@mst.edu; daryl@mst.edu).

Jianmin Zhang, Songping Wu, Ming-Feng Xue, Chi Kin Benjamin Leung, and Eric A. MacIntosh are with the Google LLC, Mountain View, CA 94043 USA (e-mail: jianmin@google.com; songpingwu@google.com; mingfengx@google.com; benleung@google.com; ericmac@google.com).

Color versions of one or more figures in this article are available at https://doi.org/10.1109/TEMC.2023.3280922.

Digital Object Identifier 10.1109/TEMC.2023.3280922

With the surge in MLCC usage, however, another issue has become increasingly common. The acoustic noise generated by MLCCs in consumer devices like laptops, cell phones, and wireless earbuds, gives the impression of poor product quality and impacts customer satisfaction. While the $BaTiO_3$ dielectric commonly used in MLCCs allows small sized capacitors with high value, it also has a piezoelectric effect. When an electrical signal passes through the MLCC, the MLCC will contract and expand in proportion to the signal. This vibration of the MLCC will be transferred to the PCB to which it is soldered. The MLCC piezoelectric effect is often called "singing" [3], [4].

Even though the vibration of an MLCC could be small, there could be dozens to hundreds of MLCCs on the PCB which collectively can create a large "speaker" area and noticeable noise. As a result, the PDN may not only need to be evaluated for its electrical performance, but for the acoustic noise induced by power rail noise on the MLCCs. The correlation between acoustic noise and MLCC vibration was demonstrated in [5], based on a simple test board. In [6], the acoustic noise induced by MLCCs was studied through a simulation-based investigation of the vibration behavior of the PCB. Optimizing the placement of MLCCs can reduce acoustic noise [7]. Measurement techniques to identify the primary MLCC vibration sources on a PCB were demonstrated in [8] and the relationship between the PDN noise, PCB vibration and acoustic noise were studied.

Although the correlation between the electrical noise on MLCCs and acoustic noise from the system has been demonstrated [7], [8], and a practical simulation flow for performing acoustic noise analysis has been presented [9], it is still challenging to predict the acoustic noise over a broad frequency range. Previous studies show that frequencies where the electrical noise on the MLCCs peak correspond to those found in the acoustical noise, but do not show a firm link between the two. Both the power noise spectrum and the PCB vibration properties should be studied when analyzing acoustic noise. A simulation and validation methodology for predicting acoustic noise is proposed in the following article. The acoustic noise can be found from three properties: the PDN noise at the MLCC, the MLCC transfer function from electrical noise to mechanical force, and the vibrational response of the PCB. Acoustic noise can be mitigated by reducing any of these aspects. The PCB vibration

properties are found through simulation and considered as a system response. The overall acoustic noise is obtained by combining the electrical power spectrum seen at the MLCCs with the system response. The predicted acoustic noise shows good correlation with the measured acoustic noise, suggesting the proposed method could help engineers analyze and mitigate acoustic noise issues more effectively.

II. Acoustic Noise Mechanism and Analysis Method

A. MLCC and PCB Vibration

The deformation of MLCCs due to PDN noise causes vibrations which directly generates acoustic noise. While this noise alone is not noticeable to human ears, the MLCC vibration could be transferred to the PCB and produce audible levels of acoustic noise. The PCB response is a primary contributor to the acoustic noise induced by MLCCs. It has been demonstrated that acoustic noise could be analyzed from the vibration of the PCB in previous studies [8]. This article focuses on the simulation analyses of the PCB properties.

B. Modal Analysis and Harmonic Analysis

Modal analysis is the study of the vibration characteristics of a structure and can be used to study vibration of a PCB [8]. The analysis starts with the equation of motion

$$[M]\{\ddot{u}\} + [C]\{\dot{u}\} + [K]\{u\} = [F] \tag{1}$$

where M is the mass, $\ddot{u}$ is acceleration, C is damping, $\dot{u}$ is velocity, K is stiffness, u is displacement, and F is the applied force. As the natural frequencies and associated mode shapes are inherent properties of the structure, independent of external force, and damping has little influence on the structure's modal parameters, the equation of motion used for modal analysis of a free and undamped system can be written as follows:

$$[M]\{\ddot{u}\} + [K]\{u\} = \{0\}\ . \tag{2}$$

Assuming harmonic motion for every point of the structure, the displacement and acceleration expressions can be written as follows:

$$\{u\} = \{\phi\}_i \sin(\omega_i t + \theta_i) \tag{3}$$

$$\{\ddot{u}\} = -\omega_i^2 \{\phi\}_i \sin(\omega_i t + \theta_i)\,. \tag{4}$$

Substituting (3) and (4) into (2)

$$\left([K] - \omega_i^2 [M]\right)\{\phi\}_i = \{0\} \tag{5}$$

where ω_i^2 are the square of the natural frequencies of the structure (i.e., the eigenvalues), and $\{\phi\}_i$ is the mode shape at certain natural frequencies (i.e., the eigenvectors). $[M]$ and $[K]$ are known matrices associated with the PCB structure, so ω_i and $\{\phi\}_i$ can be determined.

The structure tends to vibrate at its natural frequencies. The modal analysis shows the locations where the structure is sensitive to an external applied force. In practice, the PCB is generally fixed to a rigid structure (e.g., the case) at several support locations. These locations need to be set properly in the mechanical model as boundary conditions to accurately calculate natural frequencies and mode shapes.

The results of modal analysis can be used to estimate the displacement of the PCB from an external applied force—in this case the vibration force of the MLCCs—to predict acoustic noise. The displacement of the board at position $\mathbf{X} = \{x,y\}$ from a unit force at the position of MLCC k located at position $\{x_k,y_k\}$ can be expressed as a linear combination of modal shapes

$$D_{k,\boldsymbol{X}}(f) = \sum_{i=1}^{n} \phi_{i,X}\{Y_{i,X}\} \tag{6}$$

where $D_{k,\boldsymbol{X}}(f)$ is the transfer function for the displacement, $\phi_{i,X}$ are the mode shapes calculated through modal analysis for an excitement at $\mathbf{X}$, $\{Y_{i,X}\}$ are the modal coordinates which will be calculated in harmonic analysis, and n is the number of modes used.

C. Total Response

In addition to the board response, the acoustical noise also depends on the vibration of the MLCCs caused by power supply noise. Here we propose to predict the total response $R_{\boldsymbol{X}}(f)$ at position $\mathbf{X}$ as follows:

$$R_{\boldsymbol{X}}(f) = \sum_{k=1}^{m} a_k(f) \cdot P_k(f) \cdot D_{k,\boldsymbol{X}}(f) \tag{7}$$

where f is frequency, $P_k(f)$ is the power supply noise at MLCC k, $a_k(f)$ is a transfer function between the electrical noise (in watts) at MLCC k to the force generated by the MLCC, and the total response is determined from a summation of the displacement caused by all MLCCs on the board, m. Here, the transfer function $a_k(f)$ will be assumed to have a uniform value over the frequency range of interest for simplicity, as the aim of the study is to estimate the frequency response of the acoustic noise, rather than estimate its actual value.

III. Simulation and Validation on a Real Product

A. Modal Analysis of PCB

The device under test (DUT) investigated in this article was a PCB from a wireless earbud. The PCB consists of eight copper layers with FR-4 dielectric in between. The mechanical model of the PCB is shown in Fig. 1. All components were included and are modeled as rectangular or cylindrical blocks, including individual RLC components, ICs, connectors, and microphones.

The material density, volume, and Young's modulus of the PCB and the mounted components are critical to accurately determining the mechanical response of the system. The dielectric material in the PCB was modeled as a uniform structure with density 1.85 g/cm^3 and Young's modulus 20 GPa. As modeling the copper traces directly would require a small mesh size and many elements, the copper layers were modeled as uniform layers with an appropriate mix of copper and FR4, and the equivalent density and Young's modulus was calculated accordingly. The parameters for the components were obtained from vendors and datasheets.

The PCB under study was fixed to the shell of the earbud with glue at four locations. Four fixed supports were added to the sides

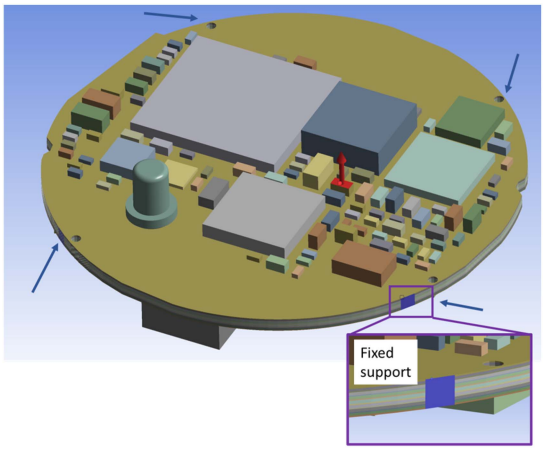

Fig. 1. Mechanical model of the PCB. Blue arrows indicate the locations of fixed support. The red arrow indicates the location of the external force added to the dominant MLCC to simulate the board response. The inset shows an expanded view of one of the fixed supports.

TABLE I
FIRST EIGHT MODAL FREQUENCIES OF THE DUT

Mode	Frequency [Hz]	Mode	Frequency [Hz]
1	8417	5	23 681
2	11 756	6	30 547
3	13 093	7	35 871
4	17 822	8	38 385

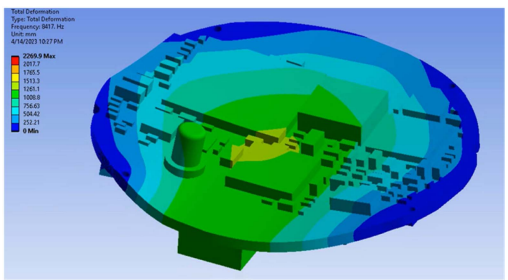

(a)

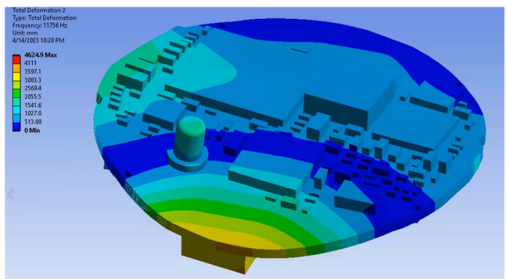

(b)

Fig. 2. Modal shapes associated with (a) mode 1 and (b) mode 2.

of the PCB at similar locations, as shown by the blue arrows in Fig. 1. These fixed supports were the boundary conditions for modal analysis.

Simulation of the first eight modes gave the natural frequencies shown in Table I. The first and second natural frequencies are 8417 and 11 756 Hz, respectively. The modal shapes for these frequencies are shown in Fig. 2. Because the structure

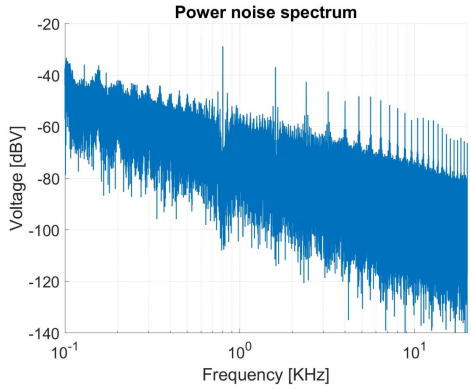

Fig. 3. Power noise spectrum of the dominant MLCC.

tends to vibrate at the natural frequencies, higher acoustic noise is expected at these frequencies.

B. Harmonic Analysis of PCB

The power noise at the MLCCs is needed to determine the total PCB response. While there are several MLCCs in this prototype earbud, one MLCC was found to have up to 20 dB more power noise than other MLCCs and to dominate the acoustic noise. The power noise spectrum on this MLCC is shown in Fig. 3. The measured frequency is from 100 Hz to 20 kHz, which covers the hearing range of most humans. There is a peak at 800 Hz, which is the fundamental frequency of the IC, as well as harmonics at 1600 Hz, 2400 Hz, and so on. Broadband power rail noise is also shown in the power noise spectrum.

As the power noise on one MLCC is expected to dominate the PCB response, a harmonic analysis was performed with a uniform force applied to the surface of this MLCC as shown in Fig. 1(Red arrow) in order to obtain $D_{k,\boldsymbol{x}}(f)$ as in (6). The simulation was performed from 0 to 20 000 Hz in 50 Hz steps. "Cluster results" was activated, so the software (Ansys Mechanical) could automatically increase the frequency points around the natural frequencies without missing the peaks. The force was set to 1 N for all frequencies. To avoid unrealistically high peak values at the natural frequencies, a 0.01 damping ratio was added.

The average deformation across the entire PCB found in simulation from this one MLCC is shown in Fig. 4. The frequencies that show peak deformation are matched with the natural frequencies. Below the first natural frequency, especially lower than 4 kHz, the frequency response is almost flat, which means the structure is not sensitive to vibration in this frequency range.

C. Measured Acoustic Noise and Predicted Response

The acoustic noise of the DUT was measured in a mini acoustic chamber with a very low noise floor. The measurement setup is shown in Fig. 5. An ear simulator was placed in the chamber. Ear simulators are important devices for objective evaluation of the acoustic performance of different earphones. In this setup, the earbud was placed in the ear simulator and the acoustic noise was measured while blank audio was playing.

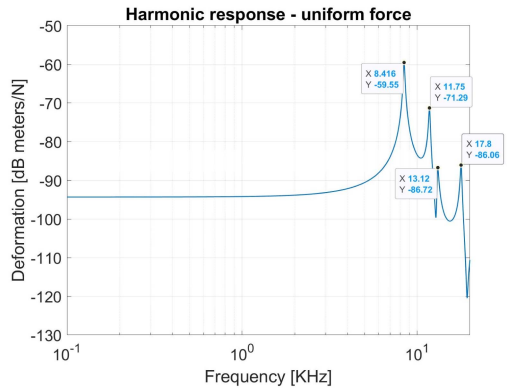

Fig. 4. Deformation of the structure.

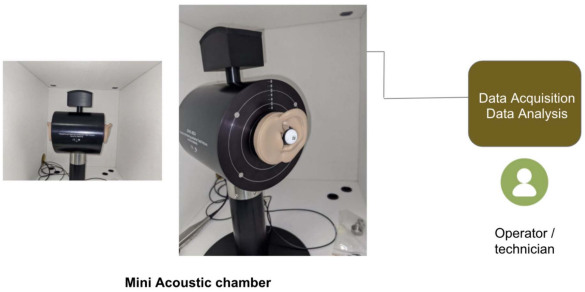

Fig. 5. Acoustic noise measurement setup.

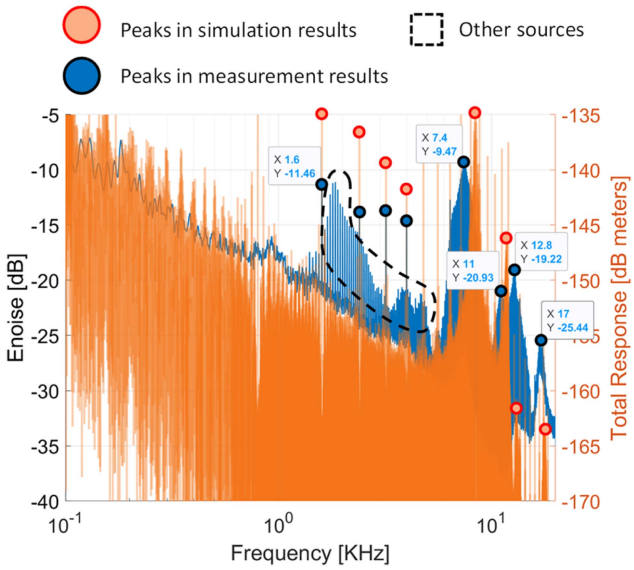

Fig. 6. Blue curve/dots: measured acoustic noise. Orange curve/dots: Average absolute displacement across the PCB predicted from noise on the dominate MLCC. Area circled with dotted line: "Other" sources of noise.

The measured acoustic noise from 100 Hz to 20 kHz is shown with the blue curve in Fig. 6. The harmonics of the 800 Hz fundamental frequency are shown in the acoustic noise measurement at 1.6 kHz, 2.4 kHz and so on. Between 1.6 and 3 kHz, there are many narrow peaks, which were shown to come from other sources but not further investigated (circled in black).

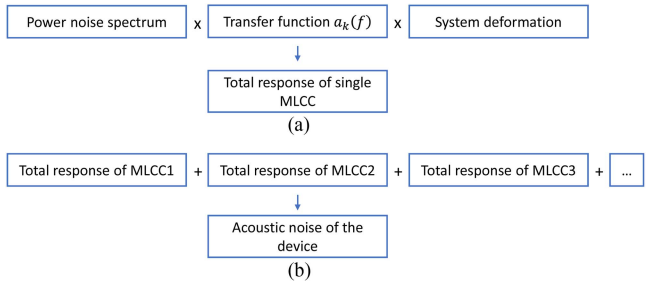

Fig. 7. Flow chart of the proposed acoustic noise analysis. (a) Total response of single MLCC. (b) Acoustic noise of the device.

TABLE II
COMPARISON OF THE BROAD PEAKS

Peaks	Prediction	Measurement
1	8.4 kHz	7.4 kHz
2	11.8 kHz	11.0 kHz
3	13.1 kHz	12.8 kHz
4	17.8 kHz	17.0 kHz

Four broad peaks are shown at 7.4, 11.0, 12.8, and 17 kHz which are most likely caused by the "singing" capacitor effect.

The displacement of the PCB caused by vibration of the dominant MLCC was estimated from the measured power noise across this MLCC and the simulated transfer function $D_{k,\boldsymbol{x}}(f)$, assuming $a_k(f) = 1$. The orange curve in Fig. 6 shows the average absolute displacement predicted across the entire PCB. The impact of the power rail noise is shown in the response. Overall, the average predicted displacement tends to follow a similar trend as the measured acoustic noise. The four broad peaks in the total response match peaks in the measured acoustic noise, as shown in Table II, though these peaks in measurement occur at somewhat lower frequencies than the predicted resonant frequencies, most likely because of the added weight of components connected to the board that were not simulated, like the shell, cables, connectors, etc. The narrow peaks which are the harmonics of the 800 Hz fundamental frequency are also shown in the total response. These results suggest that the proposed simulation method could be used to predict the frequency response of acoustic noise. While this simulation did not find the "broadband" noise, e.g., circled in black in Fig. 6, simulations were performed only for the capacitor with the largest power-supply noise.

IV. CONCLUSION

The mechanisms by which MLCCs generate acoustic noise on PCBs were studied, and a method for predicting the severity of that noise was presented. The inherent vibration properties of a PCB can be analyzed using modal analysis, and a transfer function for MLCC vibration to board response can be estimated using modal superposition. An equation predicting the PCB displacement from the MLCC/board transfer function and the MLCC power supply noise was proposed. The proposed methods were validated on a prototype earbud. The trends in the average predicted board displacement are similar

to the measured acoustic noise, with the major broad peaks in the acoustic noise found in both simulations and measurement. The proposed simulation methods show promise for analyzing the impact of singing capacitors on acoustic noise.

The proposed method demonstrates that the acoustic noise can be predicted from three components: the power supply noise at the MLCCs, the transfer function(s) that converts power supply noise into MLCC vibration, and the transfer function for system deformation resulting from the MLCC vibration. Acoustic noise could be mitigated by reducing any of these effects. The flowchart of acoustic noise analysis is given in Fig. 7.

In the DUT studied here, the power noise was worst on one MLCC which also dominated the acoustical noise, so acoustical noise was only estimated from this one MLCC. In reality, multiple MLCCs are "singing" in this design. The total response from all singing capacitors could be predicted as a superposition of each response, as indicated in (7), so long as the power supply noise is known.

In this study, the transfer function $a_k(f)$ from power supply noise at the MLCC to a vibrational force was assumed to be 1 for simplicity. With accurate $a_k(f)$, the predicted frequency response will be more accurate, and comparison of absolute values of the acoustic noise can be achieved. Better determining this transfer function is an important task for future study.

REFERENCES

[1] L. Zhang et al., "Decoupling capacitor selection algorithm for PDN based on deep reinforcement learning," in *Proc. IEEE Int. Symp. Electromagn. Compat., Signal Power Integrity*, 2019, pp. 616–620.

[2] B. Zhao et al., "Decoupling capacitor power ground via layout analysis for multi-layered PCB PDNs," *IEEE Electromagn. Compat. Mag.*, vol. 9, no. 3, pp. 84–94, Jul.–Sep. 2020.

[3] J. D. Prymak, "Piezoelectric effects ceramic chip capacitors (singing capacitors)," *Arrow Asian Times*, 2006.

[4] "Singing capacitors (piezoelectric effect)," TDK, Dec. 2006. [Online]. Available: https://product.tdk.com/system/files/contents/faq/capacitors-0031/singing_capacitors_piezoelectric_effect.pdf

[5] B. H. Ko, S. G. Jeong, Y. G. Ahn, K. S. Park, N. C. Park, and Y. P. Park, "Analysis of the correlation between acoustic noise and vibration generated by a multi-layer ceramic capacitor," *Microsyst. Technol.*, vol. 20, no. 8/9, pp. 1671–1677, Aug. 2014.

[6] Y. Sun, S. Wu, J. Zhang, C. Hwang, and Z. Yang, "Simulation methodologies for acoustic noise induced by multilayer ceramic capacitors of power distribution network in mobile systems," *IEEE Trans. Electromagn. Compat.*, vol. 63, no. 2, pp. 589–597, Apr. 2021.

[7] Y. Sun, S. Wu, J. Zhang, C. Hwang, and Z. Yang, "Decoupling capacitor layout design guidelines for acoustic noise consideration in power distribution network," in *Proc. IEEE Int. Symp. Electromagn. Compat. Signal/Power Integrity*, 2020, pp. 357–362.

[8] Y. Sun, S. Wu, J. Zhang, C. Hwang, and Z. Yang, "Measurement methodologies for acoustic noise induced by multilayer ceramic capacitors of power distribution network in mobile systems," *IEEE Trans. Electromagn. Compat.*, vol. 62, no. 4, pp. 1515–1523, Aug. 2020.

[9] X. Yan, S. Wu, M. Xue, C. K. B. Leung, D. Beetner, and J. Zhang, "A practical simulation flow for singing capacitor based acoustic noise analysis," in *Proc. IEEE Int. Symp. Electromagn. Compat. Signal/Power Integrity*, 2022, pp. 29–33.